Ellipsoid Packing Structures on Freeform Surfaces

Qun-Ce Xu[1] Bailin Deng[2] Yong-Liang Yang[1]
[1]University of Bath, UK [2]Cardiff University, UK

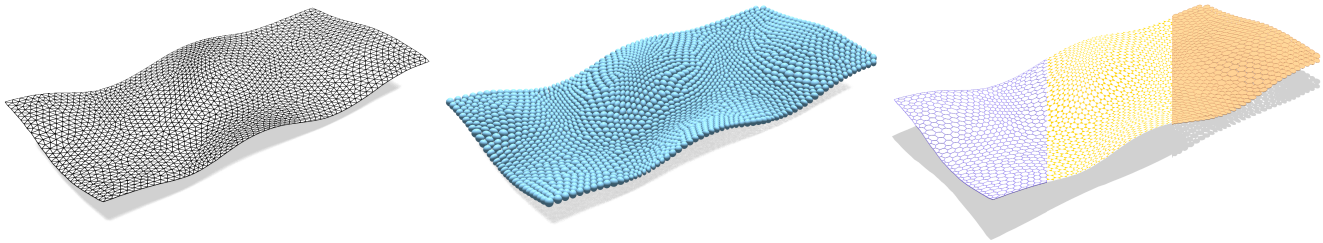

Figure 1: *We present an optimization-based framework that can generate plausible ellipsoid packing structures on freeform surfaces. The optimization is initialized by anisotropic remeshing of the underlying surface (left). The ellipsoids are densely packed on the surface and coincide with local surface features (middle). Other appealing structures can be easily derived from the ellipsoid packing structure, including hexagon-dominant mesh, hybrid mesh, and ellipse packing structure (right).*

Abstract

Designers always get good inspirations from fascinating geometric structures gifted by the nature. In the recent years, various computational design tools have been proposed to help generate cell packing structures on freeform surfaces, which consist of a packing of simple primitives, such as polygons, spheres, etc. In this work, we aim at computationally generating novel ellipsoid packing structures on freeform surfaces. We formulate the problem as a generalization of sphere packing structures in the sense that anisotropic ellipsoids are used instead of isotropic spheres to pack a given surface. This is done by defining an anisotropic metric based on local surface anisotropy encoded by principal curvatures and the corresponding directions. We propose an optimization framework that can optimize the shapes of individual ellipsoids and the spatial relation between neighboring ellipsoids to form a quality packing structure. A tailored anisotropic remeshing method is also employed to better initialize the optimization and ensure the quality of the result. Our framework is extensively evaluated by optimizing ellipsoid packing and generating appealing geometric structures on a variety of freeform surfaces.

1. Introduction

The amazing evolution of the nature has resulted in delicate geometric structures that are ubiquitous in the world, such as articulated structure of humans and animals, symmetry structure of flower petals, hierarchical structure of tree branches, just to name a few. Among all the incredible structures gifted by the nature, the structure formed by a packing of simple primitives is one of the masterpieces. As shown in Figure 2, the most well-known structure of this type is probably the honeycomb which is packed by hexagonal cells. Other examples include the compound eyes of certain insects and the turtle shells. These packing structures in nature are a rich source of inspirations for various areas in science and technology, in particular architectural design and manufacture. Figure 3 shows several real architectural buildings formed by packing primitives.

Given a freeform surface, how to computationally generate packing structures with different type of cell elements has gained signifi-

(a) (b) (c)

Figure 2: *Instances of cell packing structure in nature. (a) Honeycomb. (b) Fly's eye. (c) Turtle shell (design). Image courtesy of https://www.buzzfeed.com, http://archive.boston.com, and https://clipartxtras.com.*

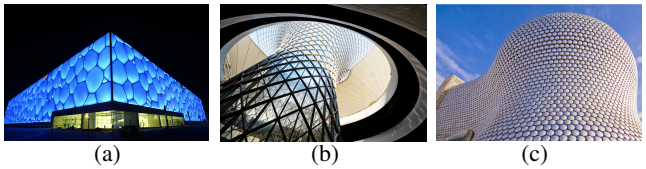

(a) (b) (c)

Figure 3: *Real architectural buildings formed by packing primitives. (a) The Water Cube in Beijing. (b) The Expo Axis in Shanghai. (c) The Selfridge Building in Birmingham. Image courtesy of https://lovelybeijing.wordpress.com, https://www.archilovers.com, and http://sidecrutex.info.*

cant attention for researchers in shape modeling and computer-aided design field [PJH*15] [WLY*16]. Schiftner et al. [SHWP09] investigated packing spheres on freeform surfaces (see Figure 4). They presented a novel structure called sphere packing mesh, which is a triangle mesh with one sphere associated at each mesh vertex, and neighboring spheres associated at each mesh edge are tangent to each other. A geometric optimization framework was devised to generate sphere packing mesh from a reference freeform surface. Interesting geometric structures such as incircle packing structure and hybrid mesh with hexagons and triangles can also be induced from sphere packing structure.

In this work, we would like to move a step further by generalizing the isotropic sphere packing structure on freeform surfaces to anisotropic case by using ellipsoids, i.e., generalized spheres, as the packing elements. The motivation of our work is two-fold and with regard to geometric design and physical fabrication respectively. First, freeform surfaces usually exhibit local anisotropy that can be described by the difference between maximal and minimal principal curvatures. By using ellipsoids, we can generate packing structures that better adapt to local surface features. Second, ellipsoid packing can simplify the fabrication process, since it enables approximation of anisotropic regions such as sharp features with a small number of long and thin ellipsoids instead of many small spheres (see Figure 5).

In order to achieve this goal, we develop an optimization framework for generating ellipsoid packing structures on freeform surfaces. We define an anisotropic metric on the surface which is adaptive to local surface features, and carefully formulate a non-linear optimization to optimize the compactness of the ellipsoids. To ensure the success of the optimization, we also propose to use anisotropic

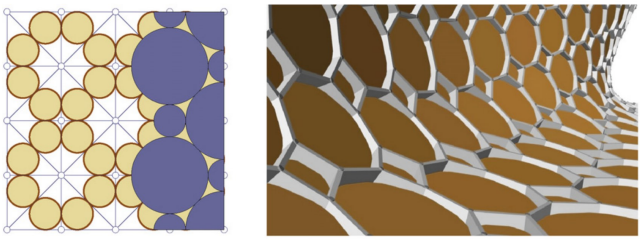

Figure 4: *2D illustration of sphere packing and incircle packing structure (left), and a hybrid polygonal structure derived from such structure. Images are adopted from [SHWP09].*

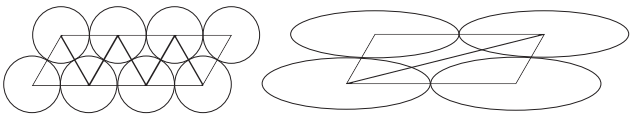

Figure 5: *Ellipsoid packing allows for approximation of anisotropic regions using fewer elements than sphere packing. Here we show a 2D example where a parallelogram is approximated by packing four ellipses instead of eight disks.*

remeshing to obtain feature-adaptive meshes to better initialize the optimization. Several interesting anisotropic structures can be derived from the ellipsoid packing structure for architectural design purpose, such as anisotropic hexagon-dominant mesh, hybrid mesh, and ellipse packing structure. We test our framework on a variety of freeform surfaces with different geometry and topology. The results demonstrate the effectiveness of our framework for generating useful ellipsoid packing structures that are adaptive to surface features.

In summary, our work makes two major contributions: i) We present the first optimization framework for generating anisotropic ellipsoid packing structure on freeform surfaces with robust remeshing-based initialization; ii) We generate a number of appealing architectural designs from ellipsoid packing structures optimized on various freeform surfaces.

2. Related Works

Here we focus on previous works that are closely related to ours, especially on packing spheres and ellipsoid on surfaces, and anisotropic remeshing techniques. Interested readers may refer to [PJH*15] for a detailed survey on general cell packing structures, and [PEVW15] for a comprehensive review on broader architectural geometry.

Sphere packing on surfaces. Sphere packing on a 3D surface and its 2D counterpart - circle packing on the plane - have gained significant research interests in the discrete differential geometry field, especially for solving surface conformal mappings [HS93] [BS04] [Ste05]. This is due to the fact that conformal mapping in the continuous case maps infinitesimal circles on the surface to infinitesimal circles, which inspires researchers to use sphere/circle packing to study discrete conformal mappings for triangulated surface. Based on the above, researchers in the geometry processing field also employed sphere/circle packings for conformal surface parameterization. Several works were presented to use sphere/circle packings to solve global conformal parameterization [JKLG08] [YGL*09] [SSP08]. The key idea is to use a sphere/circle packing to define a new metric determined by radii, and flatten the surface by changing the radii while preserving the angles between neighboring circles. However, the sphere packing structure itself and the induced structure for design purpose is not a concern. The most relevant work to ours is [SHWP09], where the authors gave detailed analysis for packing spheres on freeform surfaces represented by triangle meshes. They proposed a new type of triangle mesh called circle packing (CP) mesh, where a sphere is assigned to each vertex of the mesh and neighboring spheres associated with a mesh edge are tangential. CP

meshes are closely related to circle packing and conformal mapping since they also have an induced packing metric based on the sphere packing. The difference is that here the spheres have to be tangential, while in [JKLG08] and [YGL*09] they are allowed to intersect or be disjoint. Based on the definition of CP meshes, the authors proposed numerical optimization algorithms to generate CP mesh from a given triangle mesh. They also discussed other interesting geometric structures that can be derived from CP mesh, such as incircle packing mesh, hybrid mesh with mixed triangles and hexagons, etc., and their usage for architectural design. In this work, we would like to further explore ellipsoid packing which better coincides with the local surface anisotropy.

Ellipsoid packing on surfaces. An ellipsoid can be treated as a generalized sphere with anisotropic distance metric. However, compared with sphere/circle packing, ellipsoid packing on 3D surfaces is much less explored in the field, and is mainly used for surface remeshing. Shimada et al. [SYI00] utilized ellipsoid packing for anisotropic remeshing. A set of ellipsoids is firstly sampled on the mesh surface and repulsive forces are defined between close-by ellipsoids. Repulsion optimization is further performed to achieve an equilibrium packing. Finally Delaunay Triangulation is performed on ellipsoid centers to generate anisotropic triangulation. Note that the ellipsoids are with fixed sizes in this method, while our framework also optimizes the generalized radius of each ellipsoid, resulting in better packing structure with the additional degrees of freedom. Lo and Wang [LW05] also proposed to compute anisotropic remeshing based on ellipsoid packing. The difference is that they applied a wave-propagation method to greedily add ellipsoids on the surface, gaining efficiency but sacrificing quality. Our goal is different from the above works since we aim at high-quality ellipsoid packing that can be used for design purpose. The quality of the packing from previous work simply cannot meet our requirement due to the gaps between ellipsoids and their non-uniform distribution. Ellipsoid packing based design has been briefly discussed in the survey paper [PJH*15]. A simple extension based on generalizing the sphere packing energy in [SHWP09] is mentioned therein without either formal geometric definition of ellipsoid packing structure or special consideration on how to initialize the optimization, leading to only approximated packing that can rather be affected by insufficient initialization. We also note that Narvaez et al. [NRBV16] proposed to use ellipses to discretize a parabolic surface by parameterically elevating a planar circle packing structure. However, the method is restricted to a specific surface type and cannot be generalized to freeform surfaces.

Anisotropic remeshing. Remeshing has been an active research topic in geometry processing field. Early works mainly focused on how to generate triangle meshes with regular face shape (equilateral triangle) and valence (ideally six) [AUGA08]. Such remeshing technique is called isotropic remeshing which benefits a lot from computational geometry tools such as Voronoi Diagram and its dual Delaunay Triangulation [BCKO08]. Anisotropic remeshing aims at generating mesh elements adaptive to local surface anisotropy. One such technique is quad-dominant remeshing for generating meshes composed by almost all quadrilaterals [BLP*13]. The mesh edges and faces are usually controlled by curvature information which naturally encodes surface anisotropy. In our work, we are more interested in triangle meshes with a dense ellipsoid packing structure, which is not suitable by using quad meshes. Due to the anisotropic nature of ellipsoids, we favor anisotropic triangle meshes that are admissible for high-quality packing structure. Compared to isotropic remeshing, the key problem here is how to define an anisotropic metric (in contrast to the isotropic Euclidean metric), based on which the new mesh vertices are evenly distributed and regularly connected (in an anisotropic manner) on the original surface. Lai et al. [LZH*07] presented an anisotropic metric called feature sensitive (FS) metric, where the metric is defined in a six dimensional space (vertex position and normal). A local parameterization based remeshing technique [SAG03] was adopted to generate meshes where more triangles are distributed in the area with large normal variations. Similar 6D anisotropic metrics for remeshing were also proposed in [LB13] [NLG15], the main difference is that here Anisotropic Voronoi Diagram (AVD) [DW05] and Restricted Voronoi Diagram (RVD) [YLL*09] were used to optimize the vertex distribution and generate mesh connectivity. Zhong et al. [ZGW*13] proposed a particle based framework for anisotropic remeshing. The anisotropic metric is an extension of the Euclidean metric by using general positive definite matrices instead of the identity matrix when defining vector inner product. Further work was done in [ZSJG14] by using global conformal parameterization and performing the remeshing in 2D.

3. Triangle meshes with an ellipsoid packing

To give a formal definition of triangle meshes with an ellipsoid packing structure, we will first review the specific case of sphere packing meshes proposed in [SHWP09].

Definition 3.1. A triangle mesh $\mathcal{M}(\mathcal{V},\mathcal{E},\mathcal{F})$ is called a *sphere packing mesh* if there exists a sphere S_i with radius r_i for every mesh vertex $\mathbf{v}_i \in \mathcal{V}$, such that every pair of spheres S_i and S_j associated with mesh edge $e_{ij} \in \mathcal{E}$ are externally tangent to each other.

The tangential condition can be mathematically measured on every mesh edge e_{ij}. It is well known that two spheres S_i and S_j are externally tangent if and only if the distance between the two sphere centers is equal to the sum of their radius:

$$||\mathbf{v}_i - \mathbf{v}_j|| = r_i + r_j \tag{1}$$

Ellipsoid packing is a generalization of sphere packing since an ellipsoid is a generalized sphere as the following.

Ellipsoid as generalized sphere. A sphere can be simply represented in the following implicit form:

$$(\mathbf{p}-\mathbf{c})^T(\mathbf{p}-\mathbf{c}) = r^2, \tag{2}$$

where $\mathbf{p}$ is a point on the sphere, $\mathbf{c}$ is the center, and r is the radius. The definition of the sphere can be generalized to other dimensions, with circle as its 2D counterpart. Note that here we define distance using the Euclidean metric which is isotropic in a sense that the metric is encoded by an identity matrix:

$$\text{dist}^2(\mathbf{p},\mathbf{c}) = (\mathbf{p}-\mathbf{c})^T\mathbf{I}(\mathbf{p}-\mathbf{c}), \tag{3}$$

where $\text{dist}(\mathbf{p},\mathbf{c})$ denotes the distance between $\mathbf{p}$ and $\mathbf{c}$. If we generalize the distance metric by replacing the identity matrix $\mathbf{I}$ with an arbitrary positive definite matrix $\mathbf{M}$, then instead of a sphere we can define an ellipsoid:

$$(\mathbf{p}-\mathbf{c})^T\mathbf{M}(\mathbf{p}-\mathbf{c}) = r^2, \tag{4}$$

where the aspect ratio and the major axes are encoded in $\mathbf{M}$.

Anisotropic metric. To generate an ellipsoid packing structure, how to define $\mathbf{M}$ adaptive to local geometric features is very important, since it determines the shape and orientation of an ellipsoid. We also use local curvature tensor to define $\mathbf{M}$ since it locally measures the surface anisotropy based on principal curvatures and the corresponding directions, and is widely used in geometry processing field. More specifically, we first estimate the principal curvatures $\kappa_{max}, \kappa_{min}$ and directions $\mathbf{d}_{max}, \mathbf{d}_{min}$ using a robust local fitting based approach [DEL10] implemented in libigl [JP17]. Then the anisotropic metric $\mathbf{M}$ is defined as:

$$\mathbf{M} = \mathbf{Q}\Lambda\mathbf{Q}^T, \tag{5}$$

where $\mathbf{Q}$ is an orthogonal matrix formed by two principal curvature directions and their cross product (the normal vector $\mathbf{n}$) as:

$$\mathbf{Q} = \left[\mathbf{d}_{max}, \mathbf{d}_{min}, \mathbf{n}\right],$$

and Λ is a diagonal matrix defined based on principal curvatures.

$$\Lambda = \mathbf{Diag}\left[f(\kappa_{max}), f(\kappa_{min}), \frac{f(\kappa_{max})+f(\kappa_{min})}{2}\right].$$

It can be seen that the ellipsoid axes are aligned with the two principal directions and the normal. The lengths along individual axes are adaptive to the two principal curvatures via a mapping function f. In our implementation, we define f as:

$$f(x) = |x| + 1. \tag{6}$$

Note that for an umbilic point where $\kappa_{max} = \kappa_{min}$, the ellipsoid simply becomes a sphere. For surfaces exhibiting strong local anisotropy, we also find that it is better to use a moderate logarithmic function to avoid elongated ellipsoid as:

$$f(x) = \log(|x| + 1) + 1. \tag{7}$$

Based on the above, we now discuss how to define triangle meshes with an ellipsoid packing structure.

Definition 3.2. A triangle mesh $\mathcal{M}(\mathcal{V}, \mathcal{E}, \mathcal{F})$ is called an *ellipsoid packing mesh* if there exists an ellipsoid E_i with generalized radius r_i for every mesh vertex $\mathbf{v}_i \in \mathcal{V}$, such that every pair of ellipsoids E_i and E_j associated with mesh edge $e_{ij} \in \mathcal{E}$ satisfy the generalized equation of Eqn. 1:

$$||\mathbf{v}_i - \mathbf{v}_j|| = r_i^{\mathbf{d}_{ji}} + r_j^{\mathbf{d}_{ij}}, \tag{8}$$

where $r_i^{\mathbf{d}_{ji}}$ is the *directional radius* of ellipsoid E_i along a unit vector $\mathbf{d}_{ji} = (\mathbf{v}_j - \mathbf{v}_i)/||\mathbf{v}_j - \mathbf{v}_i||$, $r_j^{\mathbf{d}_{ij}}$ is defined similarly.

The geometric meaning of the above equation is that the two ellipsoids E_i and E_j meet at a common point on edge e_{ij}. Compared with Eqn. 1, the only difference is that instead of using constant radius of a sphere, here we use varying directional radius of an ellipsoid which is defined as below.

Definition 3.3. The directional radius $r^{\mathbf{d}}$ of an ellipsoid as defined in Eqn. 4 is the distance between the point $\mathbf{p}$ on the ellipsoid and the center $\mathbf{c}$, with $\mathbf{d} = (\mathbf{p} - \mathbf{c})/||\mathbf{p} - \mathbf{c}||$.

Proposition 3.1. For an ellipsoid defined as in Eqn. 4, the directional radius $r^{\mathbf{d}}$ and the generalized radius r satisfy the following equation:

$$r^{\mathbf{d}} = \frac{r}{\sqrt{\mathbf{d}^T\mathbf{M}\mathbf{d}}}. \tag{9}$$

Proof. Suppose $\mathbf{d} = (\mathbf{p} - \mathbf{c})/||\mathbf{p} - \mathbf{c}||$, Eqn. 4 can be re-written as:

$$(r^{\mathbf{d}}\mathbf{d})^T\mathbf{M}(r^{\mathbf{d}}\mathbf{d}) = r^2 \Rightarrow (r^{\mathbf{d}})^2(\mathbf{d}^T\mathbf{M}\mathbf{d}) = r^2,$$

then it can be seen that Eqn. 9 holds. □

3.1. Optimization algorithm

Based on the definition of ellipsoid packing mesh, we now discuss how to optimize an initial mesh $\mathcal{M}(\mathcal{V}, \mathcal{E}, \mathcal{F})$ to generate such structure, given a reference surface Φ which would be provided by the designer.

We first define an ellipsoid packing energy term f_{ep} based on Eqn. 8 to measure the quality of the ellipsoid packing structure:

$$f_{ep} = \sum_{e_{ij}\in\mathcal{E}} (||\mathbf{v}_i - \mathbf{v}_j|| - r_i^{\mathbf{d}_{ji}} - r_j^{\mathbf{d}_{ij}})^2. \tag{10}$$

Note that our definition of ellipsoid packing energy conforms to the former geometric definition of the ellipsoid packing mesh. A simpler extension based on directly generalizing the sphere packing energy in [SHWP09] is mentioned in [PJH*15], which is less accurate than the above form. A detailed discussion can be found in Appendix A.

We also adopt the same strategy in [SHWP09] to keep the optimized mesh close to the reference surface Φ. The closeness is measured in two aspects. First, the vertices of the ellipsoid packing mesh are required to be close to the the reference surface using the following energy term:

$$f_{close} = \sum_{\mathbf{v}_i\in\mathcal{V}} \mathrm{dist}(\mathbf{v}_i, \tau_{\pi(\mathbf{v}_i)})^2, \tag{11}$$

where $\pi(\mathbf{v}_i)$ is the closest point of $\mathbf{v}_i$ on the reference surface Φ, and $\tau_{\pi(\mathbf{v}_i)}$ is the tangent plane at $\pi(\mathbf{v}_i)$.

For references surface with boundary, it is also required that the boundary vertices of the ellipsoid packing mesh is close to the boundary of the reference surface:

$$f_{close}^{\partial} = \sum_{\mathbf{v}_i\in\mathcal{V}_b} \mathrm{dist}(\mathbf{v}_i, T_{\tilde{\pi}(\mathbf{v}_i)})^2, \tag{12}$$

where $\tilde{\pi}(\mathbf{v}_i)$ is the closest point of $\mathbf{v}_i$ on the boundary $\partial\Phi$ of the reference surface, and $T_{\tilde{\pi}(\mathbf{v}_i)}$ is the tangent vector at $\tilde{\pi}(\mathbf{v}_i)$.

The overall objective function is a weighted sum of packing and closeness terms:

$$F = \lambda_1 f_{sp} + \lambda_2 f_{close} + \lambda_3 f_{close}^{\partial}, \tag{13}$$

where $\lambda_1 = 0.5, \lambda_2 = 10, \lambda_3 = 10$. We choose weights according to the typical setting, i.e., higher weights for penalty terms (10 for surface/boundary closeness). Given the initialization is good, we simply use the same weights without tuning for all experiments.

Numerics.
The above optimization is a non-linear least-squares problem, which we solve using the Levenberg-Marquardt algorithm implemented in the Ceres library [AMO18]. Also, since the all the terms are

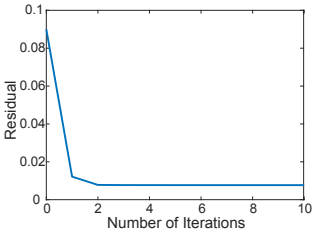

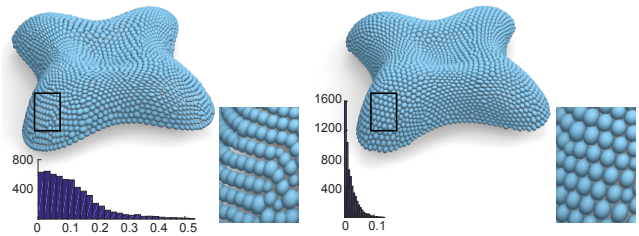

Figure 6: *Ellipsoid packing structure before and after optimization. The histograms highlight the effectiveness of the optimization for reducing packing error δ_{ij} (see Eqn. 16) for each mesh edge e_{ij}.*

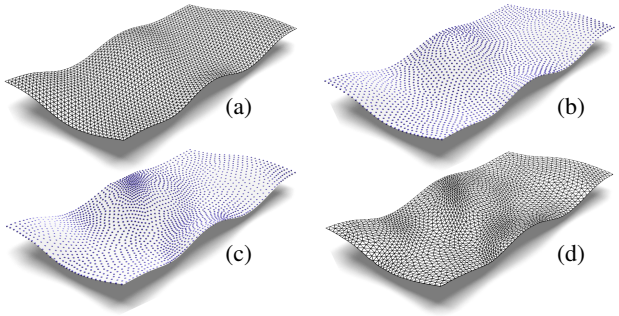

Figure 7: *We exploit anisotropic remeshing to better initialize the optimization.*

defined locally (either on mesh edge or mesh vertex), it allows efficient computation using a sparse representation. An example of ellipsoid packing optimization is shown in Figure 6. And the convergence of the optimization is demonstrated in the inset figure.

Optimization initialization. The optimization is formulated based on locally minimizing the objective function from an initial mesh. As a result, the mesh structure has a big impact on the success of the optimization. For sphere packing case, the relation between sphere packing mesh and conformal mapping is discussed based on conformal equivalent class [SHWP09]. It shows that disk-topology meshes are easy to optimize since the the conformal equivalent class (with dimension zero) is just determined by the mesh. On the other hand, meshes with complicated topology (genus and/or boundary number larger than one) are much more challenging due to the variation within a higher dimensional conformal equivalent class. Therefore the optimization is sensitive to the combinatorics of the mesh. To solve this, Centroid Voronoi Diagram (CVD) based remeshing [LWL*09] is performed to generate an isotropic mesh for such cases to make sure that the optimization succeeds.

In our scenario, since the ellipsoid packing structure conforms to surface anisotropy, we employ a tailored anisotropic remeshing method to generate a good initial mesh adaptive to local surface features for successful optimization (detailed in the next section).

Note that besides the vertex positions $\mathbf{v}_i$, the generalized radius r_i for ellipsoid E_i centered at $\mathbf{v}_i$ also needs to be optimized. To initialize r_i, we consider all the faces in the one-ring neighborhood of $\mathbf{v}_i$. For each face f_{ijk}, we compute $\hat{r}_i$, $\hat{r}_j$, and $\hat{r}_k$ such that Eqn. 8 holds for all three face edges. Then r_i is initialized as the average of $\hat{r}_i$'s over all incident faces of $\mathbf{v}_i$.

4. Anisotropic Remeshing for Packing Initialization

To better initialize the ellipsoid packing for successful optimization, we perform anisotropic remeshing conforming to the anisotropic metric used to define ellipsoid packing structure to generate good initial meshes. Given an input reference surface mesh $\mathcal{M}_0$ which discretizes Φ (see Figure 7(a)), we also adopt a particle repulsion optimization idea as in [LZH*07] [ZGW*13] to sample new mesh vertices and optimize their distribution. More specifically, we first generate new vertices randomly on $\mathcal{M}_0$ (see Figure 7(b)). This is done by randomly picking a triangle $f_{lmn} \in \mathcal{F}_0$ and creating a random sample in it. The probability of picking triangle f_{lmn} is proportional to its area. Then we define the repulsion force between close-by new vertices $\mathbf{v}_i$ and $\mathbf{v}_j$ as:

$$R_{ij} = e^{-d_{ij}^2}, \tag{14}$$

where d_{ij} is the anisotropic distance in-between:

$$d_{ij} = (\mathbf{v}_i - \mathbf{v}_j)^T (\mathbf{M}_i + \mathbf{M}_j)(\mathbf{v}_i - \mathbf{v}_j)/2. \tag{15}$$

The vertex location is updated by a gradient descent type optimization, where every vertex iteratively moves along the joint repulsion direction from other vertices by a small step length. The process ends when all the vertices are close to equilibrium (see Figure 7(c)).

After generating anisotropic mesh vertices, the next step is to construct mesh connectivity between vertices (see Figure 7(d)). Instead of using AVD and RVD [ZGW*13], we exploit the local parameterization approach similar to [LZH*07]. This is for robust remeshing of flat shapes with sparsely distributed new vertices, which cannot be properly handled using RVD [YBZW14], but is very likely to be the case for architectural design. This approach is based on a divide-and-conquer strategy. It iteratively extracts disk-topology sub-regions on $\mathcal{M}_0$, maps the sub-region to 2D via parameterization, then performs 2D Delaunay triangulation to construct mesh connectivity, and finally maps the connectivity back to 3D. Conflicting edges that may appear in overlapping area are resolved by Delaunay edge flipping. Differing from previous work, when computing mean value parameterization of a local disk domain, we use our curvature-adaptive metric other than the FS metric. In rare cases where the triangle inequality does not hold for our metric, we use FS metric instead for local parameterization. Note that our method can be used to handle meshes with arbitrary topology (i.e., varying genus and boundary number), and does not require different embedding spaces as for global parameterization [ZSJG14].

5. Derived Structures

The optimized ellipsoid packing mesh enables the derivation of appealing anisotropic structures for design purpose, generalizing those isotropic forms as presented in [SHWP09]. For clarity, we simply show 2D illustrations as in Figure 8. More results in 3D can be found in Section 6.

Anisotropic hexagon-dominant structures. It is straightforward

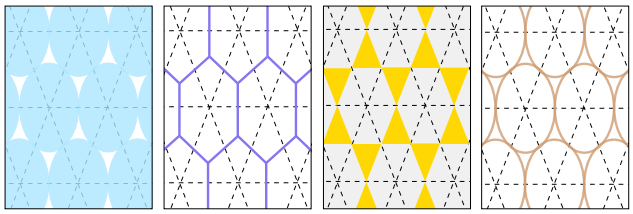

Figure 8: *Ellipsoid packing structure can derive other appealing structures for design purpose.*

to derive such dual structures from ellipsoid packing meshes (see Figure 8(b)). For realizing architecture in practice, this type of structure reduces the complexity of fabricating nodes where several beams meet together, since the valence of each (inner) mesh vertex is three, which is less than quad meshes and triangle meshes [PEVW15].

Anisotropic hybrid triangle-hexagon structures. Hybrid meshes mixed with triangles and hexagons (mostly) can also be derived in an anisotropic manner. Here we first compute the contact point $\mathbf{p}_{ij}$ of two neighboring ellipsoids (E_i and E_j) for each mesh edge e_{ij}, which is well defined after the optimization. By connecting the contact points (on edges) in mesh faces and in a one-ring neighborhood of mesh vertices, we can easily construct an anisotropic hybrid structure (see Figure 8(c)). Due to the involvement of triangles, such structure can be used to generate planar and convex hexagons in negatively curved areas of a surface, while non-convex faces are required there for pure planar hexagonal meshes.

Ellipse packing structures. We can also derive interesting ellipse packing structures adaptive to local surface features. Specifically, we create an ellipse for each mesh vertex $\mathbf{v}_i$ by fitting to all its incident contact points $\mathbf{p}_{ij}$ (as mentioned before) in a one-ring neighborhood. Due to the high quality of ellipsoid packing, the derived ellipses also form a good packing structure (see Figure 8(d)).

6. Results

We test our optimization framework on a number of freeform surfaces with varying geometry and topology complexity. A gallery of ellipsoid packing structures and derived structures on architectural and algebraic surfaces can be found in Figure 12. Our framework can also handle general shapes with complicated geometry. Figure 9 demonstrates the results on the Stanford bunny. Here we also show two ellipsoid packing structures with different levels of anisotropy by adjusting the logarithm base (4 and 2 respectively, smaller base results in elongated ellipsoids) in the moderate function (see Eqn. 7, the default base is e).

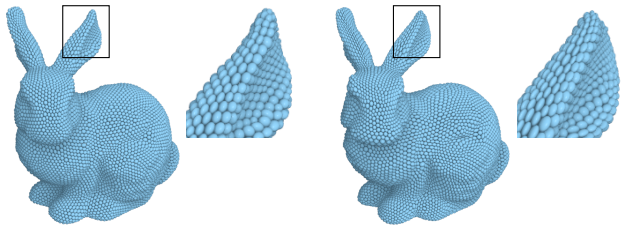

Figure 9: *Ellipsoid packing structures with moderate (left) and elongated (right) ellipsoids on the Stanford bunny model.*

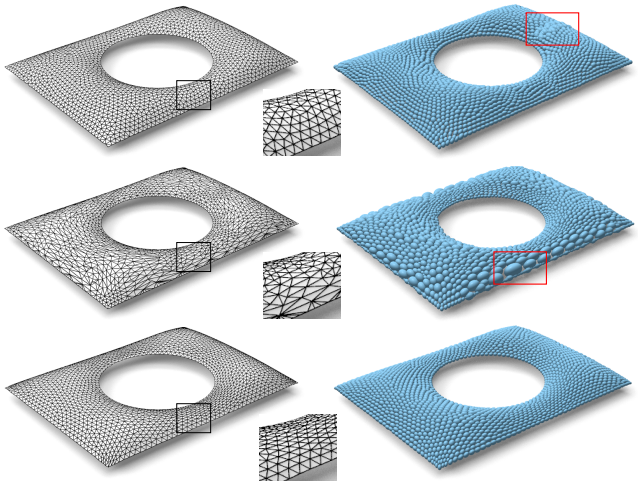

Figure 10: *Comparison between ellipsoid packing structure optimized from different initial meshes with roughly 2000 vertices. From top to bottom, the three rows show ellipsoid packing optimization results from isotropic mesh [YLL*09], irregular mesh [GH97], and anisotropic mesh (Section 4) respectively.*

To evaluate the effectiveness of the remeshing-based initialization, we compare the optimization results using initial meshes representing the same freeform surface but with different combinatorics, including isotropic mesh generated by [YLL*09], irregular mesh generated by simplifying the isotropic mesh by [GH97], and anisotropic mesh generated from Section 4. As shown in Figure 10, only anisotropic mesh results in successful optimization. As shown in the red highlighted region, isotropic mesh leads to unsolvable region with conflicting ellipsoids. Irregular mesh causes large ellipsoid shape variations that can easily affect packing compactness.

We also compare our ellipsoid packing structure with the result generated from the simple extension of sphere packing energy as mentioned in [PJH*15]. For clarity, we also show histogram of

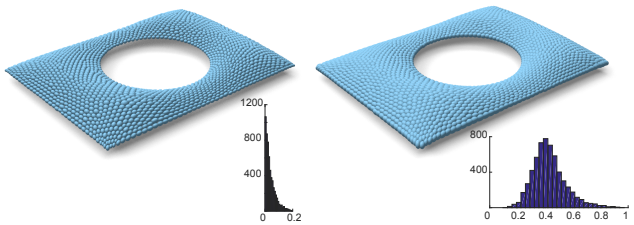

Figure 11: *Comparison between our method (left) and the simple extension in [PJH*15] (right).*

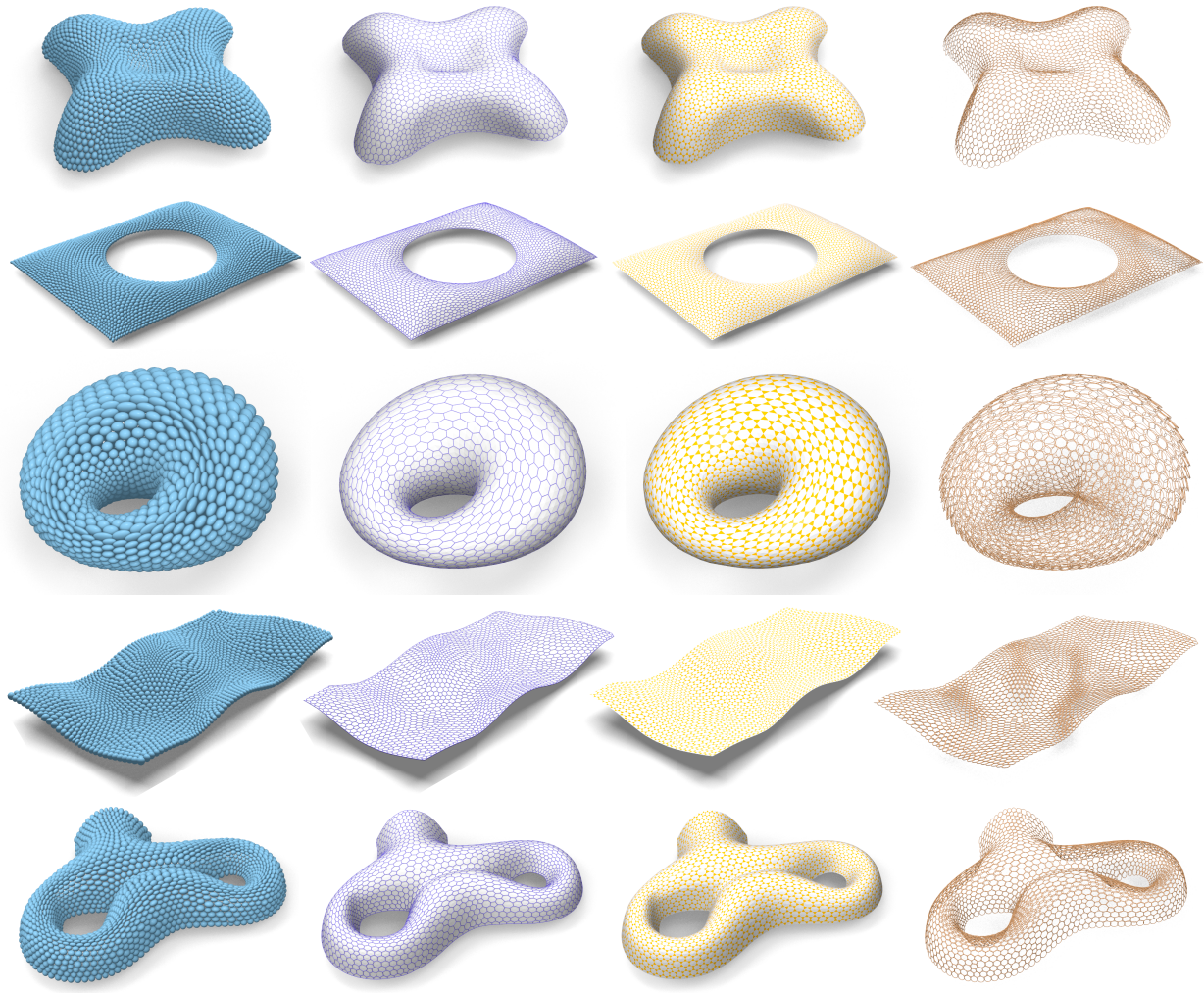

Figure 12: *A gallery of 3D ellipsoid packing and derived structures (same order as in Figure 8) on different freeform surfaces.*

per-edge packing quality measurement δ_{ij} based on Eqn 8:

$$\delta_{ij} = |1 - \frac{r_i^{\mathbf{d}_{ji}} + r_j^{\mathbf{d}_{ij}}}{||\mathbf{v}_i - \mathbf{v}_j||}|. \tag{16}$$

Figure 11 demonstrates the advantage of our approach since our optimization is based on accurately defined packing condition. Note that the result of [PJH*15] appears to be more compact but neighboring ellipsoids severely overlap (as explained in Appendix A). Our approach generates ellipsoids that are in good contact (gaps and overlaps are both penalized based on Eqn. 8).

The benefit of ellipsoid packing over sphere packing in terms of fabrication is shown in Figure 13. Fewer ellipsoids than spheres are required for the packing structure as the underlying anisotropic mesh better approximates the reference surface with fewer vertices/triangles compared with isotropic mesh, resulting in considerable material deduction when fabricating the induced ellipse packing structure using metal wires (see also Figure 5).

Performance. Our framework is implemented in C++ on a Windows laptop with 2.8 GHz CPU and 8 GB memory. For a typical model with 2000 vertices, the anisotropic remeshing and optimization take 93.3 seconds and 4.7 seconds respectively with non-optimized codes. The number of mesh vertices to be optimized play a major role for the computational efficiency, since it determines the problem scale of the remeshing and the subsequent optimization. Besides, the reference surface mesh based on which the remeshing and optimization are performed also affects the running time, as it regularizes the scope of remeshing and optimization.

Limitation and discussion. Although our framework can generate a high-quality packing of ellipsoids with good contacts, the neighboring ellipsoids are not exactly tangent to each other. The tangency between two ellipsoids is more complicated than the sphere case. Two ellipsoids can be tangent to each other while the point of tangency does not lie on the line segment L connecting the two ellipsoid centers. Such case would cause a big gap region around L which

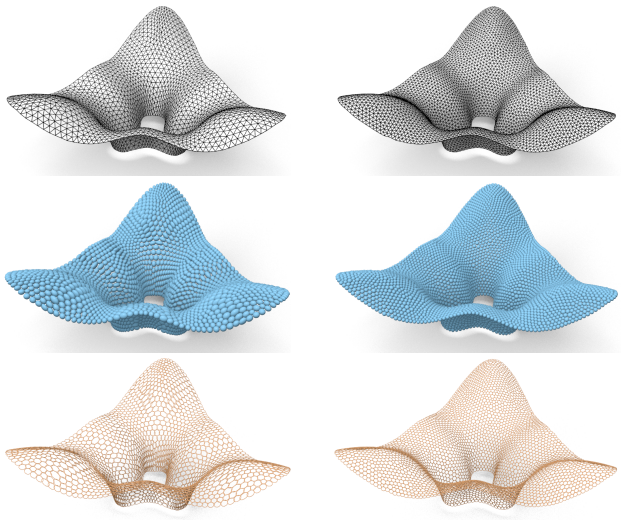

Figure 13: *Comparison between our method (left) and sphere packing (right) in [SHWP09]. To approximate the reference surface with the same Hausdoff distance (0.0012), anisotropic mesh (top left) only requires 2100 vertices, while isotropic mesh (top right) needs 4000 vertices. This results in a packing structure with less ellipsoids (middle left) than spheres (middle right), which can largely reduce the physical material by 25% (total wire length 287.4 vs. 358.3) when fabricating the induced ellipse packing structure (bottom left) compared with circle packing structure (bottom right).*

damages the compactness of the packing and makes it difficult to generate good derived structures (e.g., hybrid mesh in Figure 8). Therefore, instead of exact tangency, we only require good contact between two ellipsoids along L, as described by Eqn. 8, which is also a nice generalization from the sphere case.

Becides, our packing optimization is based on a local optimization approach (Levenberg-Marquardt algorithm) so the result may be trapped into local minimum, thus there is no guarantee of free of conflict (as shown in Figure 10 top row) between neighboring ellipsoids. This motivates us to devise a good initialization strategy which takes into account surface anisotropy. We do not see any failure case for the freeform surfaces we tested in the paper.

7. Conclusion and Future Work

In this paper, we present a computational framework for generating anisotropic ellipsoid packing structures on freeform surfaces. Compared with previous work, our packing structure is intrinsic to local surface anisotropy and adaptive to surface features. The key of our approach is a carefully designed formulation which accurately measures the packing quality. Non-linear optimization is utilized with good initialization to generate plausible ellipsoid packing structures with good quality. Several other appealing anisotropic structures can also be derived to benefit architectural design. The experiments and comparisons demonstrate the performance of the presented framework on freeform surfaces with varying geometry and topology.

In the future, we would like to investigate the relationship between ellipsoid packing with Quasi-conformal mapping [ZLYG09] [WMZ12], which maps infinitesimal circles to ellipses. This might help initialize the ellipsoid packing on surfaces by mapping circles from 2D parameter domain. How to specify the mapping such that the ellipsoids still coincides with local surface features is worth exploring. Also, in addition to geometric design, we would like to take into account the physical behavior of the derived structures such as involving supporting beams for real fabrication consideration.

Acknowledgements

We are grateful to the anonymous reviewers for their comments and suggestions. We thank Shi-Min Hu, Yu-Kun Lai, Peter Hall, and Christian Richardt for helpful discussions. The models used in the paper are courtesy of Caigui Jiang, Alexander Schiftner, and Johannes Wallner. The work was supported by CAMERA, the RCUK Centre for the Analysis of Motion, Entertainment Research and Applications, EP/M023281/1.

Appendix A:

The survey paper [PJH*15] only briefly discussed ellipsoid packing by directly generalizing the following sphere packing energy in [SHWP09]:

$$f_{sp} = \sum_{e_{ij}\in\mathcal{E}} [\mathrm{dist}(\mathbf{v}_i,\mathbf{v}_j)^2 - (r_i+r_j)^2]^2, \tag{17}$$

where the distance between $\mathbf{v}_i$ and $\mathbf{v}_j$ is measured using the isotropic distance metric $\mathrm{dist}(\mathbf{v}_i,\mathbf{v}_j)^2 = (\mathbf{v}_i-\mathbf{v}_j)^T\mathbf{I}(\mathbf{v}_i-\mathbf{v}_j)$ as in Eqn. 3. The simple extension is to replace isotropic distance by anisotropic distance. But due to the anisotropic distance metric associated with two neighboring ellipsoids are usually different in general, the anisotropic distance between $\mathbf{v}_i$ and $\mathbf{v}_j$ is simply measured as the average of the two anisotropic distances with respect to $\mathbf{v}_i$ and $\mathbf{v}_j$:

$$\mathrm{dist}'(\mathbf{v}_i,\mathbf{v}_j)^2 = \frac{\mathrm{dist}_{\mathbf{v}_i}(\mathbf{v}_i,\mathbf{v}_j)^2 + \mathrm{dist}_{\mathbf{v}_j}(\mathbf{v}_i,\mathbf{v}_j)^2}{2}. \tag{18}$$

In the above equation, $\mathrm{dist}_{\mathbf{v}_i}(\mathbf{v}_i,\mathbf{v}_j)^2 = (\mathbf{v}_i-\mathbf{v}_j)^T\mathbf{M}_i(\mathbf{v}_i-\mathbf{v}_j)$, $\mathrm{dist}_{\mathbf{v}_j}(\mathbf{v}_i,\mathbf{v}_j)^2 = (\mathbf{v}_i-\mathbf{v}_j)^T\mathbf{M}_j(\mathbf{v}_i-\mathbf{v}_j)$, where $\mathbf{M}_i$ and $\mathbf{M}_j$ are the isotropic distance metrics defining the two ellipsoids E_i and E_j centered at $\mathbf{v}_i$ and $\mathbf{v}_j$ respectively. And the ellipsoid packing energy analogous to Eqn. 17 is defined as:

$$f_{ep} = \sum_{e_{ij}\in\mathcal{E}} [\mathrm{dist}'(\mathbf{v}_i,\mathbf{v}_j)^2 - (r_i+r_j)^2]^2, \tag{19}$$

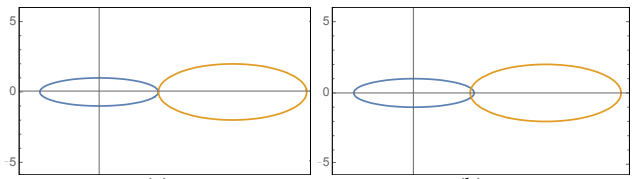

(a) (b)

Figure 14: *(a) Two ellipses are tangential to each other. (b) By enforcing Eqn. 18 , they intersect with each other.*

However, it can only describe approximated packing other than accurate packing. Here we use a simple example in 2D to demonstrate this (see Figure 14). It is easy to see that enforcing the constraint $\text{dist}'(\mathbf{v}_i,\mathbf{v}_j)^2-(r_i+r_j)^2=0$ cannot guarantee that two neighboring ellipsoid are in good contact with each other. In this simple case they even intersect. This inspires us to define a more accurate ellipsoid packing energy in Eqn. 10 based on the formal definition of ellipsoid packing mesh in Eqn. 8

References

[AMO18] AGARWAL S., MIERLE K., OTHERS: Ceres solver. http://ceres-solver.org, 2018. 4

[AUGA08] ALLIEZ P., UCELLI G., GOTSMAN C., ATTENE M.: *Recent Advances in Remeshing of Surfaces*. Springer Berlin Heidelberg, 2008, pp. 53–82. 3

[BCKO08] BERG M. D., CHEONG O., KREVELD M. V., OVERMARS M.: *Computational Geometry: Algorithms and Applications*, 3rd ed. ed. Springer-Verlag TELOS, 2008. 3

[BLP*13] BOMMES D., LÉVY B., PIETRONI N., PUPPO E., SILVA C., TARINI M., ZORIN D.: Quad-mesh generation and processing: A survey. *Computer Graphics Forum 32*, 6 (2013), 51–76. 3

[BS04] BOBENKO A., SPRINGBORN B.: Variational principles for circle patterns and koebeâĂŹs theorem. *Transactions of the American Mathematical Society 356*, 2 (2004), 659–689. 2

[DEL10] DANIELE P., ENRICO P., LUIGI R.: Efficient multi-scale curvature and crease estimation. In *Proceedings of Computer Graphics, Computer Vision and Mathematics* (2010), pp. 9–16. 4

[DW05] DU Q., WANG D.: Anisotropic centroidal voronoi tessellations and their applications. *SIAM Journal on Scientific Computing 26*, 3 (2005), 737–761. 3

[GH97] GARLAND M., HECKBERT P. S.: Surface simplification using quadric error metrics. In *Proceedings of the 24th Annual Conference on Computer Graphics and Interactive Techniques* (1997), SIGGRAPH '97, pp. 209–216. 6

[HS93] HE Z.-X., SCHRAMM O.: Fixed points, koebe uniformization and circle packings. *Annals of Mathematics 137*, 2 (1993), 369–406. 2

[JKLG08] JIN M., KIM J., LUO F., GU X.: Discrete surface ricci flow. *IEEE Transactions on Visualization and Computer Graphics 14*, 5 (2008), 1030–1043. 2, 3

[JP17] JACOBSON A., PANOZZO D.: Libigl: Prototyping geometry processing research in c++. In *SIGGRAPH Asia 2017 Courses* (2017), pp. 11:1–11:172. 4

[LB13] LÉVY B., BONNEEL N.: Variational anisotropic surface meshing with voronoi parallel linear enumeration. In *International Meshing Roundtable* (2013), pp. 349–366. 3

[LW05] LO S., WANG W.: Generation of anisotropic mesh by ellipse packing over an unbounded domain. *Engineering with Computers 20*, 4 (2005), 372–383. 3

[LWL*09] LIU Y., WANG W., LÉVY B., SUN F., YAN D.-M., LU L., YANG C.: On centroidal voronoi tessellation—energy smoothness and fast computation. *ACM Trans. Graph. 28*, 4 (2009), 101:1–101:17. 5

[LZH*07] LAI Y.-K., ZHOU Q.-Y., HU S.-M., WALLNER J., POTTMANN H.: Robust feature classification and editing. *IEEE Transactions on Visualization and Computer Graphics 13*, 1 (2007), 34–45. 3, 5

[NLG15] NIVOLIERS V., LÉVY B., GEUZAINE C.: Anisotropic and feature sensitive triangular remeshing using normal lifting. *Journal of Computational and Applied Mathematics 289* (2015), 225 – 240. 3

[NRBV16] NARVÁEZ-RODRÍGUEZ R., BARRERA-VERA J. A.: Lightweight conical components for rotational parabolic domes. *Advances in Architectural Geometry 2016* (2016). 3

[PEVW15] POTTMANN H., EIGENSATZ M., VAXMAN A., WALLNER J.: Architectural geometry. *Computers & Graphics 47*, C (2015), 145–164. 2, 6

[PJH*15] POTTMANN H., JIANG C., HÖBINGER M., WANG J., BOMPAS P., WALLNER J.: Cell packing structures. *Computer-Aided Design 60* (2015), 70–83. 2, 3, 4, 6, 7, 8

[SAG03] SURAZHSKY V., ALLIEZ P., GOTSMAN C.: Isotropic Remeshing of Surfaces: a Local Parameterization Approach. In *International Meshing Roundtable* (2003), pp. 215–224. 3

[SHWP09] SCHIFTNER A., HÖBINGER M., WALLNER J., POTTMANN H.: Packing circles and spheres on surfaces. *ACM Transactions on Graphics (TOG) 28*, 5 (2009), 139. 2, 3, 4, 5, 8

[SSP08] SPRINGBORN B., SCHRÖDER P., PINKALL U.: Conformal equivalence of triangle meshes. *ACM Trans. Graph. 27*, 3 (2008), 77:1–77:11. 2

[Ste05] STEPHENSON K.: *Introduction to circle packing: The theory of discrete analytic functions*. Cambridge University Press, 2005. 2

[SYI00] SHIMADA K., YAMADA A., ITOH T.: Anisotropic triangulation of parametric surfaces via close packing of ellipsoids. *International Journal of Computational Geometry & Applications 10*, 04 (2000), 417–440. 3

[WLY*16] WANG X., LE T. H., YING X., SUN Q., HE Y.: User controllable anisotropic shape distribution on 3d meshes. *Computational Visual Media 2*, 4 (2016), 305–319. 2

[WMZ12] WEBER O., MYLES A., ZORIN D.: Computing extremal quasiconformal maps. *Comput. Graph. Forum 31*, 5 (2012), 1679–1689. 8

[YBZW14] YAN D. M., BAO G., ZHANG X., WONKA P.: Low-resolution remeshing using the localized restricted voronoi diagram. *IEEE Transactions on Visualization and Computer Graphics 20*, 10 (2014), 1418–1427. 5

[YGL*09] YANG Y.-L., GUO R., LUO F., HU S.-M., GU X.: Generalized discrete ricci flow. In *Computer Graphics Forum* (2009), vol. 28, Wiley Online Library, pp. 2005–2014. 2, 3

[YLL*09] YAN D., LÉVY B., LIU Y., SUN F., WANG W.: Isotropic remeshing with fast and exact computation of restricted voronoi diagram. *Computer Graphics Forum 28*, 5 (2009), 1445–1454. 3, 6

[ZGW*13] ZHONG Z., GUO X., WANG W., LÉVY B., SUN F., LIU Y., MAO W., ET AL.: Particle-based anisotropic surface meshing. *ACM Trans. Graph. 32*, 4 (2013), 99–1. 3, 5

[ZLYG09] ZENG W., LUO F., YAU S. T., GU X. D.: Surface quasi-conformal mapping by solving beltrami equations. In *Proceedings of the 13th IMA International Conference on Mathematics of Surfaces XIII* (2009), pp. 391–408. 8

[ZSJG14] ZHONG Z., SHUAI L., JIN M., GUO X.: Anisotropic surface meshing with conformal embedding. *Graphical Models 76*, 5 (2014), 468–483. 3, 5